3 차원 놋치 및 쐐기의 응력 강도계수

이용우† • 임세영*

The intensity of a singular near-tip field around the vertex of a three-dimensional notch or wedge

Yongwoo Lee and Seyoung Im

Key Words : M-integral(M-적분); near-tip stress intensity(응력강도).

Abstract

Singular stress fields around three-dimensional wedges are examined, and the near-tip intensity is calculated via the two-state M-integral with the aid of the domain integral representation. A numerical example demonstrates the effectiveness and accuracy of the present scheme for computing the stress intensities of singular stresses near the generic three-dimensional wedges.

1. Introduction

The computation of the near-tip intensities of the singular fields may be rather straightforward for the two-dimensional wedges, and there are many schemes available(see Im and Kim[1] and the papers cited therein, for examples). The computation of the intensities for three-dimensional wedges is much more complicated in comparison to those of the aforementioned two-dimensional ones. There are many researchers that have discussed only the order of the stress singularities on three-dimensional wedge vertices. However, no systematic computational schemes have been reported regarding the calculation of the near-tip intensities of the singular stress fields around three-dimensional wedges, to the best of the author's knowledge.

†Mech. Eng., KAIST, lyw@imhp.kaist.ac.kr

*Professor, Mech. Eng., KAIST, sim@mail.kaist.ac.kr

The purpose of the present work is to report on a numerical scheme for finding the near-tip intensities around three-dimensional wedges with the aid of the two-state M-integral. A brief review is given of the eigenfunction expansion of the solution for three-dimensional elastic wedges. The two-state M-integral is applied for calculating the near-tip intensity by utilizing the complementary relationship for the eigenvalues of the three-dimensional wedges in the sense of M-integral.

For a numerical example, we choose the three-dimensional bimaterial interface corner, which was discussed by Labossiere and Dunn[2].

2. Eigenfunction expansion of the solution for three-dimensional elastic wedges

For the purpose of analysis for stress singularities at the vertex, we introduce the eigenfunction expansion (see Benthem[3], Ghahremani and Shih[4]) for the elastic solution, which is given in the form of the separable displacement field:

$$
\begin{aligned}
u &= \frac{1}{2\mu}\mathrm{Re}[\sum_{\delta_n} \beta_n r^{\delta_n+1}\tilde{u}_n(\theta,\phi;\delta_n)] \\
v &= \frac{1}{2\mu}\mathrm{Re}[\sum_{\delta_n} \beta_n r^{\delta_n+1}\tilde{v}_n(\theta,\phi;\delta_n)] \qquad (1) \\
w &= \frac{1}{2\mu}\mathrm{Re}[\sum_{\delta_n} \beta_n r^{\delta_n+1}\tilde{w}_n(\theta,\phi;\delta_n)]
\end{aligned}
$$

where r, θ and ϕ are the spherical coordinates with the origin at the vertex O, and (u, v, w) are the components of displacement in (r, θ, ϕ) directions, respectively. Values of $\lambda_n(=\delta_n+1)$, which are employed for convenience of the expression instead of δ_n+1, are called the eigenvalues and its corresponding eigenfunctions are $\tilde{u}_n(\theta,\phi;\lambda)$, $\tilde{v}_n(\theta,\phi;\lambda)$ and $\tilde{w}_n(\theta,\phi;\lambda)$.

Hence, the stress singularity occurs at the origin when $\mathrm{Re}(\lambda_n)<1$. On the other hand, the strain energy is bounded at the origin and this requires $\mathrm{Re}(\lambda_n)>-1/2$ (boundedness of strain energy requires $\mathrm{Re}(\lambda_n)>0$ for two-dimensional wedge vertices). However, $\mathrm{Re}(\lambda_n)<0$ implies that the displacement fields are unbounded at r=0, which is unrealistic except for a concentrated load applied at the vertex. Therefore, we are primarily interested in eigenvalues $\lambda_n(=\delta_n+1)$ in the range $0<\mathrm{Re}(\lambda_n)<1$.

Let the stress and strain components in the spherical coordinates be represented by 1-D arrays as follows:

$$(\sigma_1,\sigma_2,\sigma_3,\sigma_4,\sigma_5,\sigma_6)=(\sigma_{rr},\sigma_{\theta\theta},\sigma_{\phi\phi},\sigma_{\theta\phi},\sigma_{r\phi},\sigma_{r\theta}) \quad (2a)$$

$$(\varepsilon_1,\varepsilon_2,\varepsilon_3,\varepsilon_4,\varepsilon_5,\varepsilon_6)=(\varepsilon_{rr},\varepsilon_{\theta\theta},\varepsilon_{\phi\phi},2\varepsilon_{\theta\phi},2\varepsilon_{r\phi},2\varepsilon_{r\theta}) \quad (2b)$$

Material constitutive relationship is then given as

$$\sigma_i = C_{ij}\varepsilon_j \qquad (3)$$

where i, j =1~6, and C_{ij} is the material stiffness which satisfies $C_{ij}=C_{ji}$.

3. Application of two-state M-integral for 3-D wedges

The M-integral is written as[5]:

$$M = \int_S \{Wx_i n_i - t_i u_{i,k} x_k + \frac{m-n}{m} t_i u_i\} dS \qquad (3)$$

where "S" is a closed surface. Note that W and t_i indicate the strain energy density and the traction components, given as $W=\frac{1}{2}C_{ijkl}\varepsilon_{ij}\varepsilon_{kl}$ and $t_i=\sigma_{ij}n_j$. Furthermore u_i is the displacement component, and m the degree of homogeneity of the strain energy density, that is, 2 for the linear elastic problem, and n the degree of freedom of the spatial dimension, e.g., n is equal to 2 for two-dimensional domains or to 3 for three-dimensional bodies. Thus the M-integral for a three-dimensional linear elastic body is rewritten as:

$$M = \int_S \{Wx_i n_i - t_i u_{i,j} x_j - \frac{1}{2} t_i u_i\} dS \quad (i, j = 1,2,3)$$

Suppose two independent elastic states, "A" and "B". We consider another elastic state "C" obtained by superposing the two equilibrium states "A" and "B". Then the above M-integral is written as

$$M^C = M^A + M^B + M^{(A,B)} \qquad (4)$$

where the superscripts "A", "B" and "C" indicate the aforementioned elastic states, and $M^{(A,B)}$ is the two-state M-integral, given as :

$$M^{(A,B)} = \int_S [\, C_{ijkl}\varepsilon_{ij}^A \varepsilon_{kl}^B n_p x_p - (t_i^A u_{i,p}^B + t_i^B u_{i,p}^A) x_p - \frac{1}{2}(t_i^A u_i^B + t_i^B u_i^A)\,] dS \qquad (5)$$

The integral $M^{(A,B)}$ results from the mutual interaction between the two elastic states "A" and "B". This integral is referred to as the two-state *M*-integral in this context. Note that $M^{(A,B)}$ is the conservation integral for two equilibrium states since it identically vanishes for the domains with no singularities.

To explain the application of $M^{(A,B)}$ for generic three-dimensional wedges, we reconsider the conical domain in Fig. 1, where each of the two surfaces S_I and S_{II}, having the outward normal vectors, cuts through the lateral surface S_L in an arbitrary manner. Recalling that the M-integral is dependent upon the origin of the coordinate system (x_1, x_2, x_3), we take its origin at the wedge vertex. We take the closed surface $S_{II} - S_I + S_L$ where $-S_I$ means the reverse orientation of the surface S_I, that is, the same area but with the inside the region bounded by these surfaces, we can show the path independence of the M-integral as

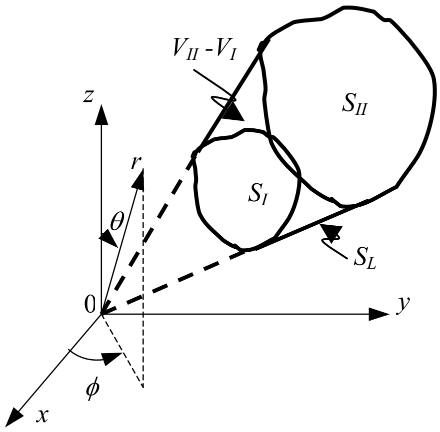

Fig. 1 The integral path for M-integral and two-state *M*-integral for three-dimensional domains.

$$M(S_I) = M(S_{II}) \qquad (6)$$

where $M(S_L) = 0$ and $M(-S_I) = -M(S_I)$ have been used. Furthermore, the path or surface independence of the two-state M-integral $M^{(A,B)}$ is apparent from the above and equation (9). That is, we have

$$M^{(A,B)}(S_I) = M^{(A,B)}(S_{II}) \qquad (7)$$

The accurate computation of the two-state integral $M^{(A,B)}$ on the far field is possible only via a regular displacement based FEM in conjunction with the volume integral for three-dimensional domains[6]. Now utilizing the domain integral and going through some manipulation, we can reach the following expressions:

$$M^{(A,B)} = -\int_{V_{II}-V_I} [\, C_{ijkm}\varepsilon_{ij}^A \varepsilon_{km}^B x_l - (\sigma_{li}^A u_{i,j}^B x_j + \sigma_{li}^B u_{i,j}^A x_j) - \frac{1}{2}(\sigma_{li}^A u_i^B + \sigma_{li}^B u_i^A)\,] q_{,l} dV \qquad (8)$$

for three-dimensional bodies, where V_I and V_{II} represent the domains bounded by S_I and S_L, and S_{II} and S_L, respectively, and $V_{II} - V_I$ indicates the region bounded by S_{II} and S_I in Fig. 1. The function $q(x_1, x_2, x_3)$ is a weight function that is defined as 1 on S_I and as 0 on S_{II} with smooth variation between S_I and S_{II}. Note that the expression (6) and (7) indicate that *M* and $M^{(A,B)}$ are conserved for an arbitrary banded volume V_{II}–V_I.

The key idea of calculating β_l is to utilize the path or surface independence property of $M^{(A,B)}$, as given in equation (7). Firstly, a convenient auxiliary state "B" is chosen, and the elastic field of the wedge under consideration is assigned to "A". $M^{(A,B)}(S_I)$ is then calculated semi-analytically on the $\theta - \phi$ domain of the spherical coordinates. We need numerical integration to evaluate the resulting integral on this domain. Next, from finite element analysis we obtain $M^{(A,B)}(S_{II})$ on the right hand side of equation (7) with the aid of the volume integral expression (8). Then equation (7) yields β_l and this value must be invariant with respect to the choice of the auxiliary elastic state as $M^{(A,B)}$ is a bilinear functional of the two elastic states "A" and "B".

The present procedure now boils downs to the choice of a convenient auxiliary state "B". For this we define a complementary eigenfield for a given eigenstate. Let the complementary eigenvalue δ_l^c of an arbitrary eigenvalue δ_l be defined in the M-integral sense as follows:

$$\delta_l + \delta_l^c = -3$$

4. Numerical Results

For a numerical example, we choose a three-dimensional wedge or three-dimensional bimaterial interface corner. Labossiere and Dunn[2] computed the stress singularity for three-dimensional bimaterial corners as shown in Fig. 2 using the finite element method. Furthermore, in this work, calculated was the near-tip stress intensity for this three-dimensional problem. In order to be able to compare our results with theirs, we choose the same three-dimensional interface corner as designed by Labossiere and Dunn[2] with the width *h*=12.5mm, and the length *L*=63.5mm in *z*-axis and the loading point distance *l*=76.2mm as shown in Fig. 2. The structure consists of 6061-T6 aluminum and cast West System 105-205 epoxy. Each material is isotropic with *E*=70.0GPa and ν=0.33 for the aluminum, and *E*=2.98GPa and ν=0.38 for the epoxy. The structure is the four-point bending specimen with the square cross section with $h \times h$ dimensions, where *h*=12.5mm as shown in Fig. 2(see Labossiere and Dunn[2] for detail).

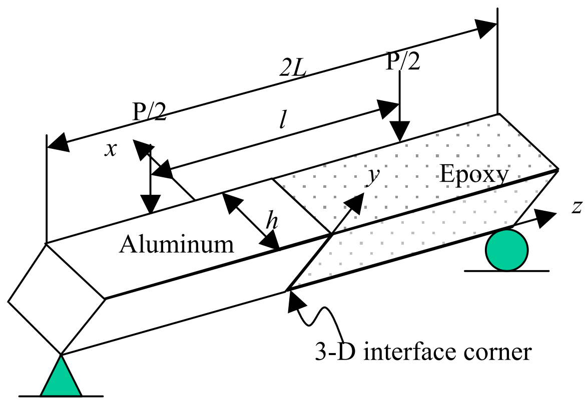

Fig. 2 Geometric configuration of three-dimensional interface corner specimen.

Labossiere and Dunn[2] proposed the asymptotic stress and a stress intensity with the stress singularity δ_s for the three-dimensional interface corner geometry as:

$$\sigma_{ij} \sim H^{3D} r^{\delta_s} \tilde{\sigma}_{ij}^{n}(\theta,\phi) \qquad (9.a)$$

$$H^{3D} = \sigma_0^{3D} h^{-\delta_s} Y^{3D}(\frac{E_1}{E_2},\nu_1,\nu_2) \qquad (9.b)$$

where *r* is the radius from the bimaterial interface corner, *h* the width as shown in Fig. 2, $Y^{3D}(\frac{E_1}{E_2},\nu_1,\nu_2)$ is a nondimensional function of the elastic mismatch. The above stress intensity H^{3D} is equivalent to the free constant β_s in Eq. (1) except that their scaling may be different from each other due to different normalization of between Eq. (1) and (9.a). They obtained Y^{3D} from fitting, using the least squares approach, the asymptotic displacements fields to the full-field displacements from the finite element solution in the vicinity of the three-dimensional interface corner along the specific rays emanating from the interface corner or vertex. Note that σ_0^{3D} is the bending nominal stress that would exist at the bottom edge of a homogeneous beam of dimension

$h \times h$ under four-point loading in Fig. 18, and is written as

$$\sigma_0^{3D} = \frac{3P(L-l)}{\sqrt{2}h^3}$$

where P is the applied loading.

The finite element mesh with 3200 twenty-node solid elements and the boundary conditions of the three-dimensional bimaterial interface corner are shown in Fig. 22. Relatively refined finite element mesh is employed near the three-dimensional bimaterial interface corner. We compute the free constant β_s using the two-state M-integral and the finite element analysis using ABAQUS, as discussed in previous section. To compare the results of Labossiere and Dunn[2] with the present results, we compute the nondimensional function Y^{3D} in equation (9.b) as tabulated in Table 2. When the nondimensional function Y^{3D} is computed, the present result is obtained using the stress singularity δ_s =-0.3586 while the result of Labossiere and Dunn[2] was obtained with the stress singularity δ_s=-0.351. The two results of the nondimensional function Y^{3D} are in good agreement. Using the free constant β_s, we obtain stress from the asymptotic solution of equation (1), and compare it with the result from the finite element analysis along the line $\theta = \pi/2$ and $\phi = \pi/4$ in Fig. 23. The finite element solution agrees well with the one term expansion (the singular term only) in the region $\rho = \sqrt{(x^2 + y^2)}$ < 0.9mm with the width h=12.5mm.

5. Conclusions

We have examined the singular stress field around a bimaterial interface corner. Moreover, we propose a general and systematic computational scheme for computing the singular stress states near the three-dimensional vertices with the aid of the two-state M-integral and the eigenfuntion expansion. We first verify numerically that the eigenvalues of the given three-dimensional problem satisfy the complementarity relationship, $\delta_n + \delta_n^c = -3$, in the three-dimensional M-integral sense. This relationship and the surface independence of the two-state M-integral are applied for extracting the near-tip intensity of the singular stress fields for three-dimensional vertices. The two numerical examples demonstrate that the present scheme is effective and accurate for computing the intensities of singular stresses near the generic three-dimensional wedges.

Reference

(1) Im, S., and Kim, K. S, 2000, “An application of two-state M-integral for computing the intensity of the singular near-tip field for a generic wedge,” J. Mech. Phys. of Solids, Vol. 48, pp. 129-151.

(2) Labossiere, P. E. W. and Dunn, M. L., 2001, “Fracture initiation at three-dimensional bimaterial interface corners,” *J. Mech. Phys. Solids*, Vol. 49, pp. 609-634.

(3) Benthem, J. P., 1977, “State of stress at the vertex of a quarter-infinite crack in a half-space,” *Int. J. Solids Struct.*, Vol. 13, pp. 479-492.

(4) Ghahremani, F. and Shih, C. F., 1992, “Corner singularities of three-dimensional planar interface cracks,” *ASME J. Appl. Mech.*, Vol. 59, pp. 61-68.

(5) Knowles, J. K. and Sternberg, E., 1978, “On a class of conservation laws in a linearized and finite elatostatics,” *Arch. Rat. Mech. Anal.*, Vol. 44, pp. 187-211.

(6) Li F. Z., Shih F. C. and Needleman A., 1985, “A comparison of methods for calculating energy release rates,” *Eng. Fract. Mech.*, Vol. 21, pp. 405-421.

Table 1 Complementary pairs of eigenvalues of the three-dimensional bimaterial interface corner.
($\delta_n + \delta_n^c = -3$)

Eigenvalue
-3.35770 ± i0.55264
-3.00016
-3.00005
-3.00000
-2.64139
-2.00028
-2.00022
-2.00003
-0.99997
-0.99978
-0.99972
-0.35861
0.00000
0.00005
0.00016
0.35770 ± i0.55264

Table 2 Nondimensional function Y^{3D} for the three-dimensional bimaterial interface corner.

	Labossiere and Dunn's results	The present results
Stress singularity	-0.351	-0.3586
Y^{3D}	0.303	0.302

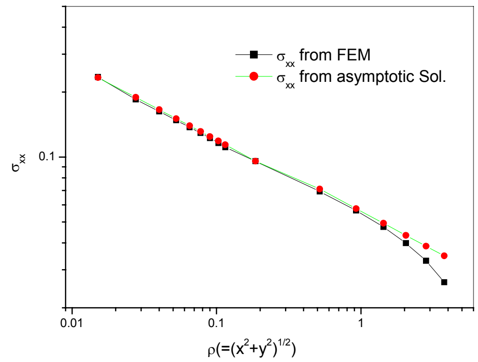

(a)

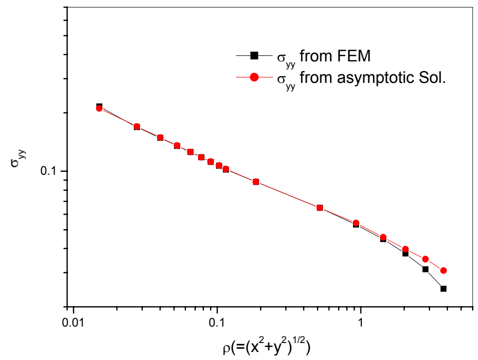

(b)

Fig. 3 Stresses versus distance from the vertex of the interface corner along $\theta = \pi/2$ and $\phi = \pi/4$ for the three-dimensional aluminum/epoxy interface corner with h=12.5mm; (a) σ_{xx}, (b) σ_{yy}.